Period of a comblike pattern controlled by atom supply and noise

Masashi Kawaguchi,[1] Hitoshi Miura,[2] Kazuhiro Kishi,[3] Masahide Sato,[4] and Makio Uwaha[1,*]
[1]*Department of Physics, Nagoya University, Furo-cho, Chikusa-ku, Nagoya 464-8602, Japan*
[2]*Department of Information and Biological Sciences, Nagoya City University, Mizuho-cho, Mizuho-ku, Nagoya, Aichi 467-8501, Japan*
[3]*Graduate School of Natural Science and Technology, Kanazawa University, Kakuma-machi, Kanazawa 920-1192, Japan*
[4]*Information Media Center, Kanazawa University, Kakuma-machi, Kanazawa 920-1192, Japan*
(Received 16 April 2014; revised manuscript received 8 October 2014; published 20 January 2015)

Pattern formation of a step on a growing crystal surface induced by a straight line source of atoms, which is escaping from the step at a velocity $V_{\rm p}$, is studied with the use of a phase field model. From a straight step, fluctuations of the most unstable wavelength $\lambda_{\rm max}$ grow. Competition of intrusions leads to coarsening of the pattern, and survived intrusions grow exponentially. With sufficient strength of the crystal anisotropy, a regular comblike pattern appears. This peculiar step pattern is similar to that observed on a Ga-deposited Si(111) surface. The final period of the intrusions, Λ, is determined when the exponential growth ends. The period depends on the strength F_u of a current noise in diffusion as $\Lambda \sim \lambda_{\rm max}|\ln F_u|$: such a logarithmic dependence is confirmed for the first time. A nonmonotonic $V_{\rm p}$ dependence of Λ indicates that the comblike pattern with a small $V_{\rm p}$ is related to an unstable growth mode of the free needle growth in a channel. The pattern is stabilized by the guiding linear source.

DOI: 10.1103/PhysRevE.91.012409 PACS number(s): 81.10.Aj, 05.70.Ln, 47.20.Hw, 68.35.Fx

I. INTRODUCTION

Atomic steps or two-dimensional crystals growing in the diffusion field show various pattern formation [1–4]. Recently a strange comblike pattern was observed in steps on a Ga-deposited Si(111) surface [5], and a similar morphology was seen in graphene films formed on a SiC substrate [6–8]. The pattern is very different from those reported previously [1–3]. The mechanism for the Si(111) case is proposed in Ref. [5] as follows. (We show a simplified model in Fig. 1, which we investigate in the present paper.) Caused by the deposition of Ga, the surface structure changes from 7×7 to $\sqrt{3} \times \sqrt{3}$ structure and, with further deposition, from $\sqrt{3} \times \sqrt{3}$ to 6.3×6.3 structure. The latter starts at the (most likely lower) step edge, and the phase boundary between $\sqrt{3} \times \sqrt{3}$ and 6.3×6.3 structures proceeds by the deposition of Ga. When the structural transition occurs, excess Si atoms are emitted to the surface from the phase boundary. Thus, for the step, an advancing source of adsorbed atoms (adatoms) is present in front. This adatom source induces growth and wandering instability of the step, which results in the comblike pattern.

We have set up a very simple model for this kind of systems (Fig. 1). A straight line source of adatoms (it is supposed to represent the structural phase boundary) is placed in front of a step and moves forward at a constant speed $V_{\rm p}$, which is proportional to the Ga deposition rate in the experiment [5]. The observed phase boundary is rather straight, which indicates its stability, and we simplify the situation by assuming the straight source. The amount of adatoms supplied onto the surface is $c_0 V_{\rm p}$ per unit time and per unit length of the linear source, where c_0 is a constant density. For simplicity we assume that diffusion of adatoms between the step and the straight source is relevant. Therefore our problem of the step morphology is equivalent to a pattern formation problem of a two-dimensional crystal in a diffusion field of atoms supplied by the escaping linear source.

To study pattern formation of steps, three types of models are widely used: discrete lattice models, continuous sharp-interface models, and phase field models. We first adopted lattice models with Monte Carlo dynamics [9,10] similar to Ref. [11]. In these studies, as well as in the present paper, a square lattice is used for simplicity. The comblike patterns are reproduced in the Monte Carlo lattice models with an escaping linear source of atoms. A step in the lattice model (LM) exhibits various morphologies from a thick comblike pattern to a thin treelike fractal pattern as the velocity of the source, $V_{\rm p}$, becomes faster. The realization of the comblike pattern relies on the crystal anisotropy. The comblike step is seen in growth towards the [11] direction, but not towards the [01] direction: growth in softer directions, but not in stiffer directions (the step stiffness $\tilde{\beta}$ is larger in the [01] direction than in the [11] direction). The characteristic length scale of the pattern is proportional to the wavelength of the initial Mullins-Sekerka instability, and the pattern shows coarsening during growth. Although the coarsening seems to proceed via competition between intrusions formed by the instability [12], the mechanism of the termination of coarsening is not known. In addition, the step patterns seem to be sensitive to fluctuations of the step. Fluctuations induce tip splitting and ultimately a fractallike pattern in the LM in an uncontrollable way [10]. Although fluctuation is necessary for the instability, it destroys the stable pattern: competition between the fluctuation and the anisotropy is the key factor for the pattern formation.

In order to find the mechanism of the termination of coarsening and the stability of the comblike pattern induced by the guiding linear source of adatoms, we make a phase field model (PM) which represents the simplified growth conditions described above. The main reason for using the PM is to perform simulations with controlling the crystal anisotropy and the noise that induces fluctuation of the step. Also, compared to the sharp interface model, the PM has the advantage that it does not require any special treatment when two steps collide or disconnect. Although in real experiments the crystal anisotropy is set by the nature of material and the strength of noise in thermal equilibrium is uniquely determined, it is our

*uwaha@nagoya-u.jp

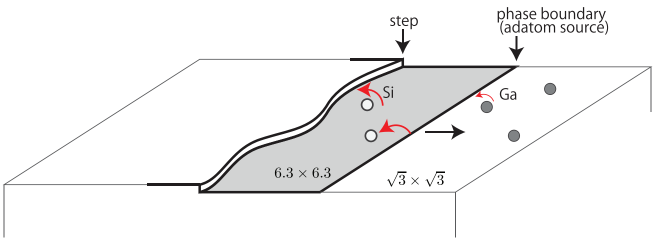

FIG. 1. (Color online) A simplified model for Ga-deposited Si(111) surface. Ga deposition expands the 6.3×6.3 area, and the phase boundary emits the excess Si atoms, which make the step grow.

purpose to control these parameters to find the mechanism of pattern fomation. The simulation model is described in Sec II.

In Sec. III, the results of our simulation are presented and analyzed. We show the change of morphology of a step with the change of the source velocity V_p and the strength of crystal anisotropy in Sec. III A. The characteristic length (the period of intrusions) Λ of the comblike pattern for slow V_p is compared with that in the LM in Sec. III B. Taking account of the effect of the noise, we discuss the coarsening process of the pattern in Sec. III C. For a fast V_p, the V_p dependence of Λ changes remarkably. This behavior is compared with the crystal growth problem in a narrow channel [13], and the stability of the pattern is discussed in Sec. III D. We summarize our results in Sec. IV.

II. PHASE FIELD MODEL

The PM we adopt here is similar to that of Refs. [14,15]. Instead of evaporation and impingement of adatoms [16], a moving straight line source in front of the step supplies adatoms. To simplify the situation, we consider only two atomic planes, the lower terrace $z = 0$ and the upper terrace $z = a$, where a is the lattice constant.

Although the experiment [5] suggests existence of the Ehrlich-Schwoebel (ES) barrier and the LM [10] assumes this condition, we adopt a different condition in the PM for simplicity. We assume infinitely fast step kinetics in the PM with adatom supply only from the phase boundary so that the diffusion on the upper side of the step is negligible. (Small deviations from the equilibrium density for a straight step due to the Gibbs-Thomson effect vanish apart from the step on the upper terrace.) The condition corresponds to the case of the Burton-Frank-Cabrera (BCF)-type step [15] of infinitely fast kinetics without impingement and desorption of adatoms, and the extra features of step growth are neglected [17]. Therefore the motion of the step is determined by the diffusion field between the step and the straight line source, and the model is effectively one-sided (Fig. 1). Our system is equivalent to the growing two-dimensional crystal with a diffuse step. The phase field parameter takes the value $-1 \lesssim \phi \lesssim 1$. Its equilibrium values are $\phi = \pm 1$, which correspond to the two flat terraces. The value of ϕ is related to the smooth "average" height z as

$$\phi = \frac{2z}{a} - 1. \tag{1}$$

The excess of the adatom density per unit cell (here and after we use the lattice constant a as the unit of length) compared to the equilibrium one for a straight step, $c_{\rm eq}^0$, is the dimensionless density variable,

$$u = \Omega\left(c - c_{\rm eq}^0\right), \tag{2}$$

where $\Omega = a^2 = 1$ is the atomic area. u takes the value $0 \lessapprox u \lessapprox c_0$, where c_0 is the density at the source. In the case of Ga-deposited Si(111), $c_{\rm eq}^0$ is an unknown small value, and $c_0 \approx 0.5$ so that the linear source supplies about half of atoms for a straight step to grow at the same speed V_p [5,10]. If we apply the model to the graphene film on SiC, the density at the source, which is a single height SiC step, corresponds to $c_0 \approx 0.33$ [8,10].

Physically consistent way to incorporate crystal anisotropy and noise in the phase field model was formulated by Karma and Rappel [18,19], and we follow their prescriptions. The phase field ϕ obeys the evolution equation

$$\tau \frac{\partial \phi}{\partial t} = -\frac{\delta \mathcal{F}}{\delta \phi}, \tag{3}$$

where τ is the relaxation time and $\mathcal{F}$ is the free energy functional given by

$$\mathcal{F} = \int \left[F(\phi,u) + \frac{1}{2} W(\theta)^2 |\nabla \phi|^2 \right] dx\, dy \tag{4}$$

with the coordinate axes parallel and perpendicular to the step: x and y [Fig. 2(a)]. The local free energy F has the form

$$F(\phi,u) = f(\phi) - \lambda u g(\phi), \tag{5}$$

where

$$f(\phi) = -\frac{\phi^2}{2} + \frac{\phi^4}{4} \tag{6}$$

and

$$g(\phi) = \phi - \frac{2\phi^3}{3} + \frac{\phi^5}{5} \tag{7}$$

with λ a coupling constant. The relaxation time τ and the step (or the interface) width W are anisotropic and depend on the angle, θ, of the normal of the step to the x axis. θ is related to $\nabla \phi$ as $\theta = \tan^{-1}(\partial_y \phi / \partial_x \phi)$. The explicit form of Eq. (3) is

$$\begin{aligned} \tau(\theta) \frac{\partial \phi}{\partial t} &= -\frac{\partial F(\phi,u)}{\partial \phi} + \nabla \cdot [W(\theta)^2 \nabla \phi] \\ &\quad + \frac{\partial}{\partial x}\left[|\nabla \phi|^2 W(\theta) \frac{\partial W(\theta)}{\partial(\partial_x \phi)} \right] \\ &\quad + \frac{\partial}{\partial x}\left[|\nabla \phi|^2 W(\theta) \frac{\partial W(\theta)}{\partial(\partial_y \phi)} \right], \end{aligned} \tag{8}$$

where $\partial_x \phi = (\partial \phi / \partial x)$ and $\partial_y \phi = (\partial \phi / \partial y)$.

For simplicity and for the comparison with the LM [10], the relaxation time τ and the width W are assumed to have the square symmetry as

$$\tau(\theta) = \tau_0 \left(1 + \epsilon_4 \cos 4\theta\right)^2, \tag{9}$$

$$W(\theta) = W_0 (1 + \epsilon_4 \cos 4\theta), \tag{10}$$

where τ_0 and W_0 are constants. The strength of anisotropy ϵ_4 is a control parameter in the present study. $\tau(\theta)$ and $W(\theta)$ are related to the capillary length $d_0 = \Omega^2 c_{\rm eq}^0 \tilde{\beta} / k_{\rm B} T$ ($\tilde{\beta}$, the

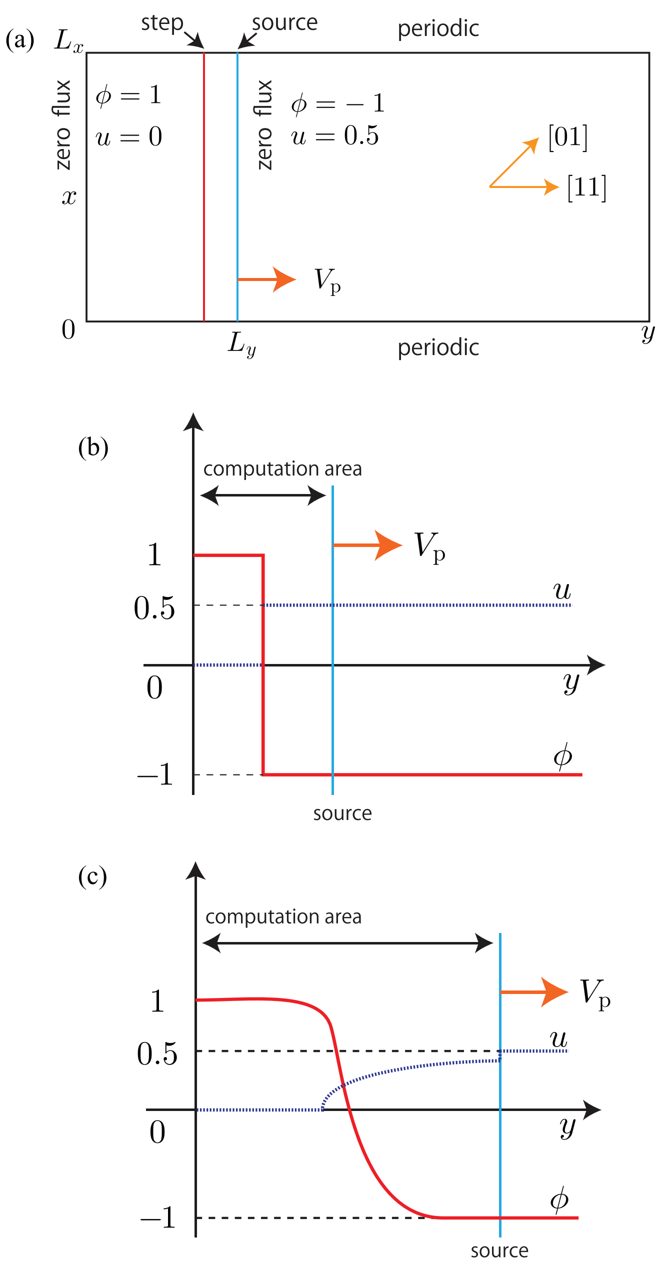

FIG. 2. (Color online) Schematic diagrams of the PM simulation. (a) Initial configuration of the system. (b) Initial profile of the fields ϕ and u. (c) Profile of ϕ and u after some advancement of the source. Computation with Eqs. (8) and (13) is performed between $y = 0$ and the position of the linear source at $y = y_{p0} + V_p t\ (=L_y)$.

step stiffness; k_B, Boltzmann constant; T, temperature) and the kinetic coefficient K as [18]

$$d_0(\theta) = \frac{a_1}{\lambda}[W(\theta) + W''(\theta)] \\ = d_0(1 - 15\epsilon_4 \cos 4\theta), \quad (11)$$

$$K(\theta)^{-1} = \frac{a_1}{\lambda}\frac{\tau(\theta)}{W(\theta)}\left[1 - a_2\lambda\frac{W(\theta)^2}{D\tau(\theta)}\right] \quad (12)$$

with $a_1 = 5\sqrt{2}/8$, $a_2 = 0.6267$, and D is the diffusion coefficient of u [see Eq. (13)]. In the growth direction $\theta = \pi/2$, the capillary length is the shortest, which implies that the growth direction corresponds to the [11] direction [Fig. 2(a)].

The density field u obeys the standard isotropic diffusion equation with a sink and noise

$$\frac{\partial u}{\partial t} = D\nabla^2 u - \frac{1}{2}\frac{\partial \phi}{\partial t} - \nabla\cdot\boldsymbol{q}. \quad (13)$$

The second term in the right-hand side represents the mass conservation in the solidification (transformation from u to ϕ, a sink term for u). The linear source is not involved in Eq. (13) because we treat the moving linear source as expanding the system size as explained later (see Fig. 2). Since we neglect evaporation and impingement of atoms, the noise is incorporated as a conserving current noise $-\nabla\cdot\boldsymbol{q}$ in Eq. (13) [19], where $\boldsymbol{q}$ is a Gaussian white noise, which satisfies

$$\langle q_\mu(\boldsymbol{r},t)q_\nu(\boldsymbol{r}',t')\rangle = 2DF_u\delta_{\mu\nu}\delta(\boldsymbol{r}-\boldsymbol{r}')\delta(t-t'). \quad (14)$$

The noise strength at thermal equilibrium is given by $F_u = \Omega^2 c_{eq}^0$ to reproduce equilibrium thermal fluctuation of the step. In general the noise strength is related to the adatom density [19] (it is related to the incomming flux for a nonconserved system [20,21]). In order to study the effect of the noise, we treat the noise strength F_u as a freely controllable parameter in our study. If the width W_0 is much smaller than the characteristic length scale of diffusion, our model corresponds to a generalized sharp step model of the BCF type with noise [15]. The stiffness of the step is anisotropic and the growth kinetics is fast [1,4].

The system consists of an initially straight step located at $y = 100$ and a linear source of adatoms in front of the step at $y = y_{p0} = 103$ [Fig. 2(a)]. The initial profiles of $\phi(y)$ and $u(y)$ are plotted in Fig. 2(b). The source starts to move away from the step with the velocity V_p releasing atoms with the density $c = c_0 + c_{eq}^0$. Such a situation is implemented in the model by expanding the area of computation: every time interval $\Delta y/V_p$ (Δy: the grid size in the y direction), new grid points with the density $u_0 = \Omega c_0$ are added to the calculation area, and then the system size is $L_x \times L_y (=y_{p0} + V_p t)$. This prescription implies constant adatom supply from the moving phase boundary, and the mass conservation across the boundary [10,12],

$$\left.\left(cV_p + D\frac{\partial c}{\partial y}\right)\right|_{L_y} = c_0 V_p, \quad (15)$$

corresponds to the boundary condition for u as $(u + (D/V_p)\partial_y u)|_{L_y} = u_0$. At the other end the zero flux condition, $\partial_y u(x,0) = 0$, is imposed. The boundary conditions for ϕ are fixed value: $\phi(x,0) = 1$, $\phi(x,L_y) = -1$. In the x direction the system is periodic: $u(x + L_x, y) = u(x,y)$, $\phi(x + L_x, y) = \phi(x,y)$. For better correspondence with our previous study of the LM [10], we choose the diffusion coefficient $D = 1$, the capillary length $d_0 = 0.05$, the width $W_0 = 3$, the time constant $\tau_0 = 299.12$, and the coupling constant $\lambda = 53.033$, which have been adjusted to make the kinetic coefficient infinity, $K(\theta)^{-1} = 0$. The spatial distance and the time increment in the numerical calculation are $\Delta x = \Delta y = 1$ and $\Delta t = 0.2$.

Since we have chosen large value of W_0/d_0, our results do not quantitatively coincide with that of the sharp interface model [22].

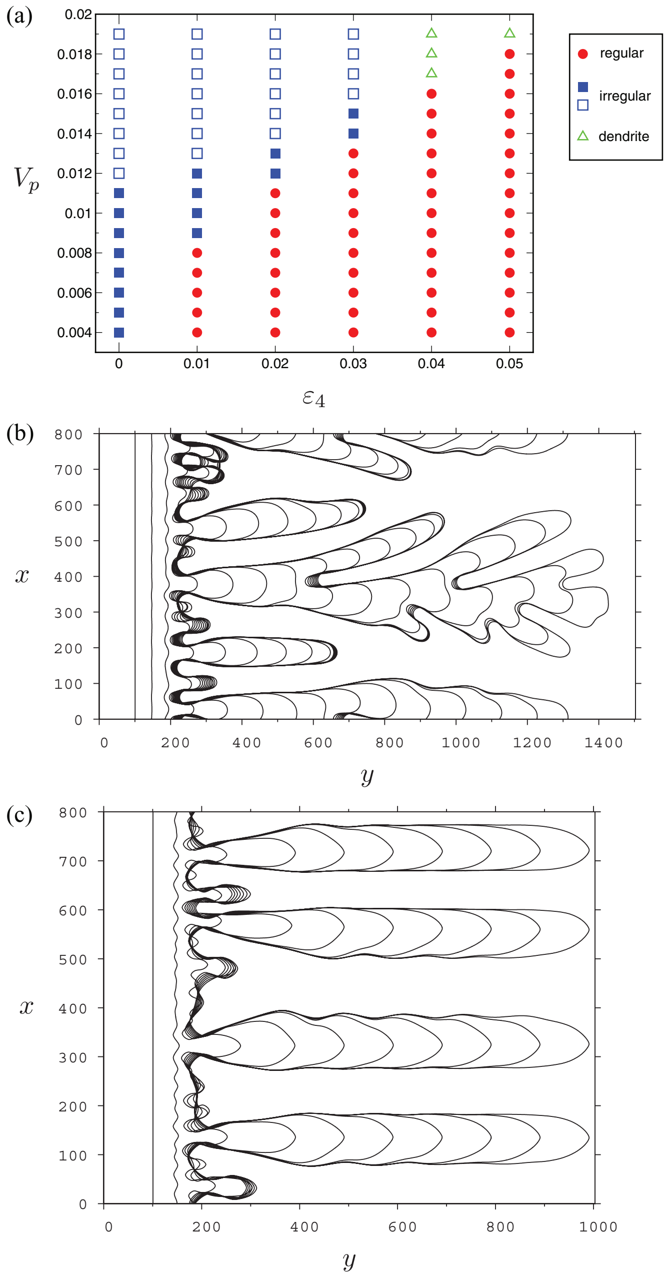

FIG. 3. (Color online) (a) Morphology diagram with the noise strength $F_u = 10^{-5}$ and the source intensity $c_0 = 0.5$. Empty symbols indicate that the step fails to follow the source. Dendrite implies pattern with side branches. (b) Irregular pattern with $V_p = 0.005$, $\epsilon_4 = 0$. (c) Comblike pattern with $V_p = 0.005$, $\epsilon_4 = 0.05$. These step patterns are superposition of the step position [defined as the contour $\phi(x,y) = 0$] at different times.

III. SIMULATION RESULTS

A. Morphology of the step

In Fig. 3(a) we summarize the results of the simulation with the noise strength $F_u = 10^{-5}$ and the source adatom density $c_0(=u_0/\Omega = u_0) = 0.5$ [23] with various values of the crystal anisotropy strength ϵ_4 and the source velocity V_p. There is a clear distinction of steps that can follow the escaping source of adatoms and that fail to follow the source, indicated by solid and empty marks, respectively. If the source is faster than a critical velocity, which depends on the crystal anisotropy, the step is left behind the source: the growth velocity is smaller than V_p. Otherwise the step follows the source, and the growth velocity coincides with V_p.

In both cases the step pattern is apparently (but not very clearly) divided into regular patterns and irregular patterns. With weak crystal anisotropy, the step becomes irregular by tip splitting of the intrusions and forms a random seaweedlike pattern like Fig. 3(b) [blue squares in Fig. 3(a)]. When the velocity of the source is slow, the irregular region shrinks. Without crystal anisotropy, $\epsilon_4 = 0$, the pattern always looks irregular even with a small V_p. In dendritic crystal growth it is known that the crystal anisotropy is necessary to make the tip stable to maintain a regular shape [24]. The anisotropy in the diffusion field produced by the source alone is not sufficient to stabilize the comblike pattern. With a stronger crystal anisotropy the tips of intrusions are stabilized. Not only splitting of the tips but also side branching is suppressed, and a regular comblike pattern like Fig. 3(c) appears [solid red circles in Fig. 3(a)]. The comblike pattern seen here is similar to that observed in the LM [10]. [Figure 3(c) corresponds to Fig. 4(d) of Ref. [10], but with less irregularity because of a weak noise. Quantitative comparison of the growth velocity is presented in Sec. III B.] It also looks similar to the pattern observed in the experiments [5–8] (see Fig. 1 of Ref. [10]). In the region of fast source velocity and strong anisotropy, the step pattern seems to develop side branches, and a dendritic pattern is seen [green triangles in Fig. 3(a)]. Stabilization of the intrusions by the anisotropy is very effective for slower velocity of the source.

The morphology change of a free dendrite has been studied by Brener, Müller-Krumbhaar, Temkin, and Ihle [25–27]. They classified the pattern into four: compact dendrite, fractal dendrite, compact seaweed, and fractal seaweed. As explained in Sec. III D, our step growth is related to free crystal growth in two dimensions. As a function of the crystal anisotropy ϵ_4, there is a resemblance between their classification and our morphology diagram of Fig. 3(a): random seaweed versus regular dendrite (comblike-pattern). However, we have not succeeded in clear distinction between various morphologies, particularly between fractal and compact morphologies. Therefore in the present paper we focus on quantitative changes within the regular comblike morphology.

B. Period of the comblike pattern compared with the LM

In our previous studies of the LM [10,12], we found that the characteristic length of the branches (the period of the pattern Λ) is several times longer than the wavelength of the initial instability, i.e., the Mullins-Sekerka wavelength $\lambda_{max} \sim 2\pi\sqrt{3Dd_0/V_p}$. The coarsening of the pattern proceeds via competition between the intrusions. Fewer and fewer intrusions survive as the initial small intrusions grow. With the increase of the source velocity, Λ and λ_{max} decrease. In other words, if V_p is large, the step follows the source by adjusting the characteristic length so as to make the diffusion length $l_D = D/V_p$ shorter.

In Fig. 4 solid symbols show the period Λ of the regular comblike pattern as a function of the source velocity V_p for

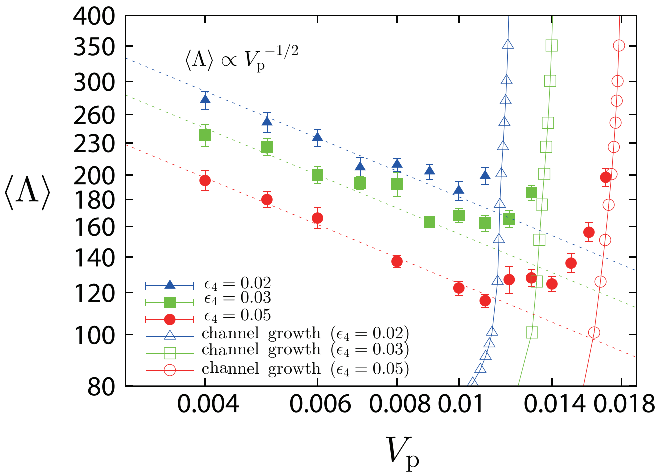

FIG. 4. (Color online) Change of the period Λ with the source velocity V_p (solid marks). The fixed parameters are $c_0 = 0.5$, $d_0 = 0.05$, $F_u = 10^{-5}$, and $L_x = 800$. The data are averaged over 20 independent runs. The velocity of a free dendrite without noise, in a channel of width Λ with $u(t = 0) = 0.5$, is plotted with empty marks (see Sec. III D).

three different values of the anisotropy parameter ϵ_4. When the source velocity is small, $V_p \lesssim 0.01$, comblike steps grow with a similar period as in the LM simulation. The period in the LM [Fig. 6(a) in Ref. [10]] is

$$\Lambda \approx \frac{10}{\sqrt{V_p}}, \tag{16}$$

for the kink energy $\varepsilon/k_B T = 2.0$, which corresponds to the capillary length $d_0(11) = c^0_{eq}\,\tilde{\beta}(11)/k_B T = 0.05 \times 1.23 = 0.061$ (we have assumed the value $c^0_{eq} = 0.05$). The period in the PM with $\epsilon_4 = 0.03$ (green squares in Fig. 4) is

$$\Lambda \approx \frac{17}{\sqrt{V_p}}. \tag{17}$$

The parameter value corresponds to the capillary length $d_0(11) = d_0(1 - 15\epsilon_4) = 0.05 \times (1 - 0.45) = 0.0275$. The capillary length is shorter in the PM, but Λ is slightly longer. Considering that the noise is much stronger in the LM, the shorter Λ in the LM is reasonable (see Sec. III C). We think that the two completely different models give essentially the same result for the step pattern when the velocity of the source is small. Now we look at how the coarsening from λ_{max} to Λ occurs, and how the noise affects the period of the final pattern.

C. Coarsening of the pattern and the noise

To study the effect of noise we perform simulation with various noise strength. Time evolution of the step pattern is shown in Fig. 5. It is evident that the period of the pattern is smaller with a stronger noise. It should be noted that the starting time of the wandering instability is earlier with a stronger noise, but the initial period of the instability is not much different.

In Fig. 6 the period of intrusions in the comblike pattern, $\langle\Lambda\rangle$, averaged over 20 runs, is shown as a function of the noise

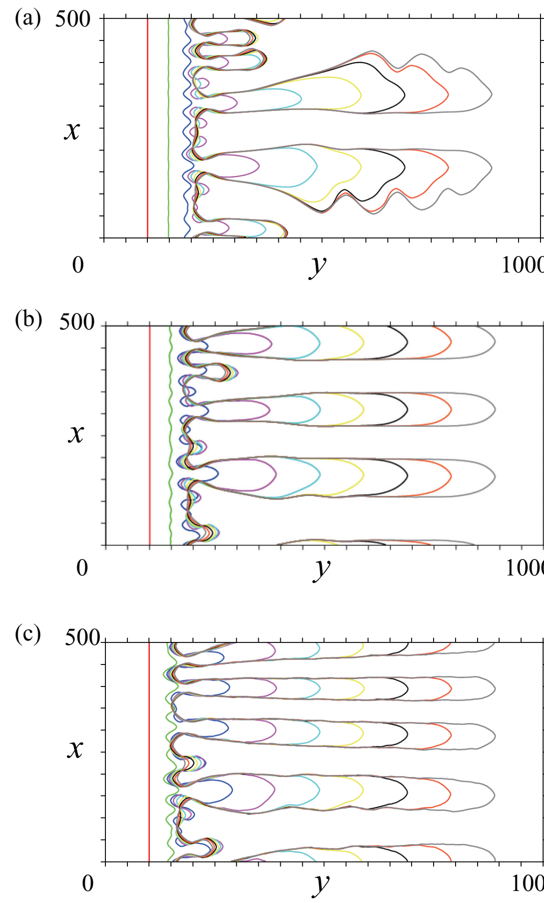

FIG. 5. (Color online) Time evolution of a comblike step with $\epsilon_4 = 0.05$ and $V_p = 0.005$ under different intensity of the noise (a) $F_u = 10^{-7}$, (b) $F_u = 10^{-5}$, and (c) $F_u = 10^{-3}$. Time increment of the successive curves is 2×10^4.

strength F_u. It depends on F_u as

$$\langle\Lambda\rangle = 7.93|\ln F_u| + 80.9, \tag{18}$$

for the source velocity $V_p = 0.005$ and the anisotropy strength $\epsilon_4 = 0.05$. The process of coarsening is the same as that in the LM [12]. In the competition for growth, fewer and fewer

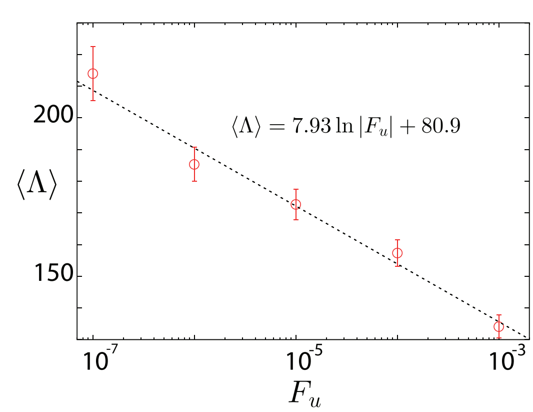

FIG. 6. (Color online) The period Λ and the strength of the noise F_u with $c_0 = 0.5$, $V_p = 0.005$, and $\epsilon_4 = 0.05$.

intrusions survive, and the distance between them increases (Fig. 5).

We attribute the logarithmic dependence to the exponential growth of the fastest intrusions as follows. Without the instability the distance between the straight step and the guiding source increases with time as $(1 - c_0)V_p t$. Once the instability occurs, the amplitude of the fastest intrusions grows exponentially at the rate $\omega_{\max} = \frac{2}{3}k_{\max}V_s$, i.e., $\delta y \sim e^{\omega_{\max} t}$, where $V_s = c_0 V_p$ is the velocity of the straight step and $k_{\max} = \sqrt{V_s/(3Dd_0)}$ is the wave number of the fastest growing mode in the linear stability analysis [9,10]. As intrusions compete for growth, only the fastest ones grow exponentially while more and more intrusions stop growing, leading to the coarsening of the pattern. The exponential growth stops when the fastest intrusions catch up with the escaping source at time τ, i.e.,

$$(1 - c_0)V_p\tau \approx \delta y_{k_{\max}}(t_0)e^{\omega_{\max}\tau}, \tag{19}$$

where $\delta y_{k_{\max}}$ is the amplitude of the fastest growing mode and t_0 ($t_0 \ll \tau$) the time at which the instability sets in. The length $(1 - c_0)V_p\tau$ determines the length of the highest intrusions of the step pattern when the coarsening ends.

The initial amplitude of the fastest growing mode, $\delta y_{k_{\max}}(t_0)$, can be estimated with the height correlation function

$$G(x,t) = \langle (y(x + x',t) - y(x',t))^2 \rangle, \tag{20}$$

where $y(x,t)$ is the location of the step position defined by $\phi[x,y(x)] = 0$ [the largest value is used if $y(x)$ is multivalued]. Since the step is initially straight, $G(x,t)$ is evaluated by looking at roughening due to the noise (see the Appendix). The amplitude of the fluctuation at t_0 is estimated by putting $(\delta y_{k_{\max}})^2 = G(\lambda_{\max},t_0)$. Since the fluctuation induced by the current noise $\boldsymbol{q}$ in our system has both conservative and nonconservative characters for the step, we cannot obtain a definite formula of $G(x,t)$. However, in any case $G(\lambda_{\max},t_0)$ is proportional to the noise strength F_u/d_0 and the amplitude of the relevant step fluctuation at t_0 must also be proportional to F_u/d_0.

It is natural to assume that the length scale necessary for the catch-up is the same as the period of the pattern: $(1 - c_0)V_p\tau \approx \Lambda$. Taking the dominant contributions for a given c_0, Eq. (19) gives the relation between the period and the strength of the noise as

$$\Lambda \sim \lambda_{\max}|\ln F_u| + \text{const.} \tag{21}$$

Such a logarithmic dependence on the noise intensity of the wavelength has been proposed in a context of morphology diagram [25], where a stable tip radius is related to the noise strength in a similar way as in Eq. (18). The idea has not been confirmed in the numerical study [26]. Figure 6 is the first clear demonstration of the logarithmic dependence on noise, which strongly suggests the above period selection scenario via the exponential growth of initial fluctuations.

Coarsening of the step pattern has been studied for step wandering as well as for step bunching [1,2,4]. For the case of step wandering five types may be distinguished: (i) chaotic behavior with a fixed wavelength (during growth with adatom evaporation [11,28]); (ii) a regular asymmetric pattern with a fixed wavelength (with electromigration which breaks inversion symmetry [29]); (iii) a $\sqrt{t}$ increase in the amplitude with a fixed wavelength (during growth without evaporation [30], or under several other circumstances [31]); (iv) a perpetual increase of the wavelength and the amplitude (during growth without evaporation with an elastic repulsion [32], or on a vicinal face of alternating surface structures with electromigration [33]); and (v) an interrupted increase of the wavelength and a perpetual increase of the amplitude (during growth with anisotropy [34]). The present step pattern is the v, that is, so-called interrupted coarsening [35]. Danker *et al.* derived a nonlinear evolution equation for a conserved system with anisotropic step stiffness (and/or an anisotropic edge diffusion) and demonstrated the interrupted coarsening. Although our step has the same anisotropy, the present system is not represented by the same nonlinear equation. We think the proposed mechanism of coarsening for the comblike pattern is different from that of Ref. [34].

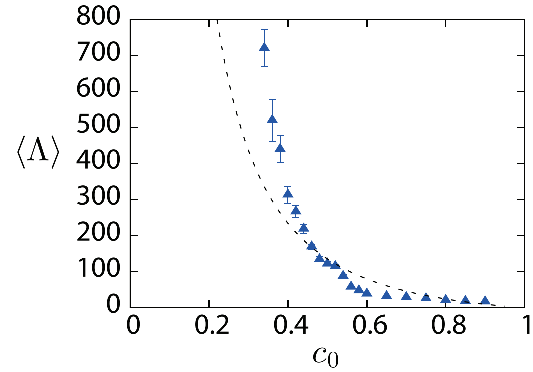

FIG. 7. (Color online) Change of the period Λ with the density at the source c_0, for $V_p = 0.01$ in a system of the size $L_x = 800$. The noise and the anisotropy are $\epsilon_4 = 0.05$ and $F_u = 10^{-5}$, respectively. The dashed line is from Eq. (19).

To check our scenario of coarsening, we also perform simulation with various densities at the source, c_0 $(=u_0)$. Figure 7 shows the simulation results of Λ as a function of c_0 for the source velocity $V_p = 0.01$ and the system size $L_x = 800$. It also shows the theoretical curve obtained from Eq. (19), by substituting the parameter values,

$$\Lambda = \delta y_{k_{\max}}(t_0)\exp\left(\frac{0.172\, c_0^{3/2}\Lambda}{1 - c_0}\right). \tag{22}$$

In the figure the initial amplitude is arbitrarily put $\delta y_{k_{\max}}(t_0) = 10^{-5}$ (the feature of the curve is insensitive to this value). The simulation results exhibit little coarsening for $c_0 \gtrsim 0.7$ and a very strong increase in Λ as c_0 is decreased, in fair agreement with the theory. With $V_p = 0.01$ the steady growth seems possible for the density region $0.35 \lesssim c_0$, but for $c_0 \lesssim 0.32$, V_p seems to exceed the limit and the step fails to follow the source [37].

D. Comblike pattern at a high speed

In Fig. 4 if the velocity of the source is fast, $V_p \gtrsim 0.01$, the period Λ starts to increase in contrast to the LM, in which a fine fractal structure is seen [10,36]. In the PM the large interface width W does not allow short wavelength structures, and the intrusions fail to follow the fast source. If the number

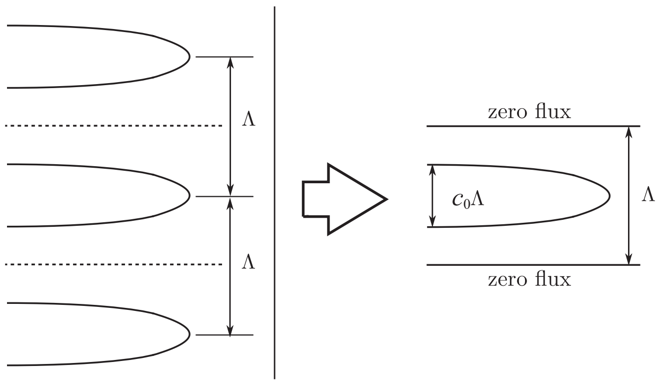

FIG. 8. The comblike pattern guided by the source (left) and a needle pattern in a channel (right).

of intrusions is reduced via competition, fewer large intrusions can grow faster and follow the source with a wider surrounding area. The maximum velocity V_p^{max} attained in such a way is the boundary between the empty symbols and the solid symbols in Fig. 3(a).

When the linear source escapes away from the step, a wide area of uniform density c_0 remains between the source and the step, and free dendrites (or needles) can grow. The maximum velocity is determined by the velocity of a free needle (dendrite) step growing in a uniform density c_0. If one cuts out a single period of the system, it corresponds to a needle (dendrite) step growing from a constant density adatoms in a channel (Fig. 8). In Fig. 4, the velocity V of a needle step growing from a uniform density c_0 in a channel of the width Λ is also plotted with empty marks (the data are the result without noise). The asymptotic behavior of V_p and Λ of the comblike step in the region $0.01 \lesssim V_p$ looks similar to the relation between V and Λ of a free needle in the channel: periodic intrusions in the present system are asymptotically equivalent to the array of free needles in a channel.

The high value limit of V_p for the solid circles in Fig. 4 corresponds to the boundary $V_p^{max}(\epsilon_4)$ between the solid red circles and the empty triangles in Fig. 3. Since the period Λ increases as V_p approaches the maximum velocity V_p^{max}, there are two steady step patterns of the same period and growing at different speed. An example of the step patterns is shown in Fig. 9. The two step patterns look similar, but the velocities differ by more than threefold. A careful observation finds that the tips are rounder and more distant from the source in the high-speed pattern [Fig. 9(b)]. The two steady states of the same period and the different velocity may be related to the two branches of the analytical solution of channel growth obtained by Brener, Geilikman, and Temkin (Fig. 3(a) in Ref. [13]). Note that the low-speed branch of the solution of channel growth, whose velocity is proportional to Λ^{-2}, is unstable [13]. This is because intrusions can grow faster by splitting themselves so that decreasing Λ. In the present model, however, the guiding linear source makes such comblike patterns grow stably by limiting the growth speed. It has been shown in the LM [12] that with a sudden change of V_p the step adjusts its velocity by tip splitting or by thinning out the intrusions. The transition of step pattern is induced by step fluctuations, which compete with the stabilizing anisotropy, and peculiar metastability of the pattern is observed.

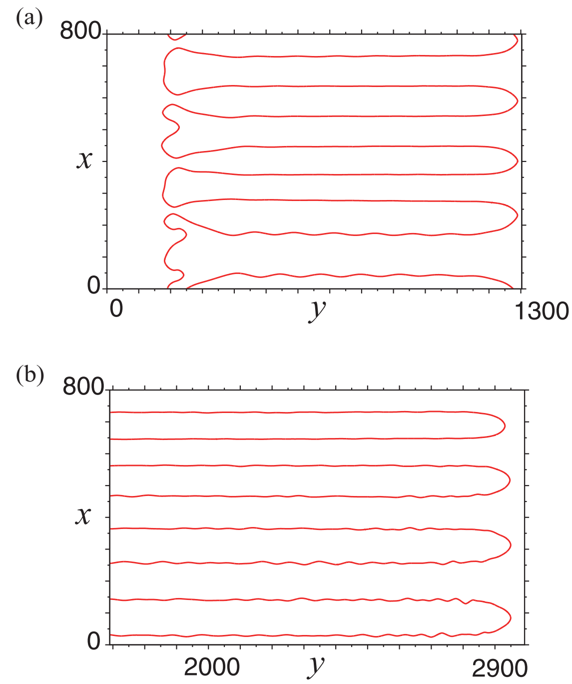

FIG. 9. (Color online) Comblike steps of the same period growing with (a) $V_p = 0.005$ and (b) $V_p = 0.017$. The red line is the position $\phi(x,y) = 0$, and the source is at the right end.

IV. SUMMARY

We constructed a phase field model of step growth with a guiding linear source, and studied effects of the adatom supply, the crystal anisotropy and the noise. A tentative morphology diagram with the strength of the anisotropy and the velocity of the source is presented. The detailed analysis of the morphology diagram is a theme of our future study. With crystal anisotropy, regular comblike patterns, similar to the one observed during Ga deposition on a Si(111) vicinal face [5], appear in accordance with the LM [10]. The logarithmic dependence of the period Λ on the noise strength F_u has been confirmed for the first time. The relation of Λ, F_u, and c_0 suggests the mechanism of interrupted coarsening of the comblike pattern. The exponential growth of the survived intrusions settles in steady growth when the step catches up with the escaping source. The height of the intrusions at the time determines the length scale of the system. If the source velocity V_p is increased to the maximum velocity that the step can follow, in contrast to the fractal growth found in the LM [10], a rapid increase in Λ occurs. The relation between the velocity and the period is reminiscent of the analytic solution [13] found in needle growth in a channel. In our step growth, the linear source stabilizes the unstable growth mode by suppressing the tip splitting of intrusions.

ACKNOWLEDGMENTS

This work was supported by JSPS KAKENHI Grants No. 24540318 and No. 26103515.

APPENDIX: ROUGHENING OF A STEP

We suppose that time evolution from the straight step obeys the Mullins-type relaxation equation with nonconserved shot noise (incomming flux) and/or conserved current noise along the step. Then the step position $y(x,t)$ may be described by

$$\frac{\partial y}{\partial t} = -\nu \frac{\partial^4 y}{\partial x^4} - \Omega \frac{\partial j}{\partial x} + \eta, \qquad \text{(A1)}$$

where $\nu = d_0 D_\mathrm{s}$ (D_s: the diffusion coefficient of the step), j is a conservative current noise (diffusive noise [20]) with the correlation

$$\langle j(x,t) j(x',t')\rangle = 2 f_j \delta(x-x')\delta(t-t'), \qquad \text{(A2)}$$

and η is a nonconservative shot noise with

$$\langle \eta(x,t)\eta(x',t')\rangle = 2 f_\eta \delta(x-x')\delta(t-t'). \qquad \text{(A3)}$$

Since the noise in our system is the conservative current noise on the surface and the step is growing with incomming flux from the surface, the noise on the step will have both conservative and nonconservative characters. Solving Eq. (A1) with the initial condition $y(x,0) = 0$ by Fourier transformation [21] we obtain

$$y_k(t) = \int_0^t dt' e^{-\nu k^4 (t-t')} (-ik\Omega) j_k(t') \qquad \text{(A4)}$$

or

$$y_k(t) = \int_0^t dt' e^{-\nu k^4 (t-t')} \eta_k(t'). \qquad \text{(A5)}$$

From Eq. (A2) or from Eq. (A3) the height correlation is

$$\langle y_k(t) y_{-k}(t)\rangle = \Omega^2 f_{j\,(\eta)} \frac{1-e^{-2\nu k^4 t}}{\nu k^n}, \qquad \text{(A6)}$$

where $n = 2$ for the conservative current noise and $n = 4$ for the nonconservative shot noise. In the long run, with the conservative noise it becomes

$$\langle y_k(t) y_{-k}(t)\rangle \to \frac{\Omega^2 f_j}{\nu k^2} = \frac{\Omega^2 f_j}{d_0 D_\mathrm{s} k^2}. \qquad \text{(A7)}$$

Since $\langle y_k y_{-k}\rangle = k_\mathrm{B}T/(L_x \tilde{\beta} k^2)$ (L_x is the system size) in thermal equilibrium, the noise intensity must be $f_j^\mathrm{eq} = c_\mathrm{eq}^0 D_\mathrm{s}/L_x$, or in general we may put $f_j = c D_\mathrm{s}/L_x$.

The height correlation in the real space is calculated as

$$G(x,t) = \sum_k \langle y_k(t) y_{-k}(t)\rangle 4 \sin^2 \frac{kx}{2}$$
$$\approx \frac{F_u}{d_0} \frac{2}{\pi} \int_{-\pi/a}^{\pi/a} dk \frac{1-e^{-2\nu k^4 t}}{k^n} \sin^2 \frac{kx}{2}, \qquad \text{(A8)}$$

where a is the lattice constant (the short wavelength cutoff), $n = 2$, and we have used the correspondence of the noise in the PM and the adatom density, $F_u^\mathrm{eq} = \Omega^2 c_\mathrm{eq}^0$. With the nonconservative noise the exponent of k in the denominator becomes $n = 4$, but the coefficient cannot be determined [38].

[1] H.-C. Jeong and E. D. Williams, Surf. Sci. Rep. **34**, 171 (1999).
[2] K. Yagi, H. Minoda, and M. Degawa, Surf. Sci. Rep. **43**, 45 (2001).
[3] T. Michely and J. Krug, *Islands, Mounds, and Atoms: Patterns and Processes in Crystal Growth Far from Equilibrium* (Springer, Berlin, 2004).
[4] For a theoretical review see C. Misbah, O. Pierre-Louis, and Y. Saito, Rev. Mod. Phys. **82**, 981 (2010).
[5] H. Hibino, H. Kageshima, and M. Uwaha, Surf. Sci. **602**, 2421 (2008).
[6] M. L. Bolen, S. E. Harrison, L. B. Biedermann, and M. A. Capano, Phys. Rev. B **80**, 115433 (2009).
[7] T. Ohta, N. C. Bartelt, S. Nie, K. Thürmer, and G. L. Kellogg, Phys. Rev. B **81**, 121411(R) (2010).
[8] H. Hibino, S. Tanabe, S. Mizuno, and H. Kageshima, J. Phys. D: Appl. Phys. **45**, 154008 (2012).
[9] M. Sato, S. Kondo, and M. Uwaha, J. Cryst. Growth **318**, 14 (2011); The boundary condition of this model is different from the explained one, and we do not adopt it here.
[10] S. Kondo, M. Sato, M. Uwaha, and H. Hibino, Phys. Rev. B **84**, 045420 (2011).
[11] Y. Saito and M. Uwaha, Phys. Rev. B **49**, 10677 (1994).
[12] S. Kondo, M. Kawaguchi, M. Sato, and M. Uwaha, J. Cryst. Growth **362**, 6 (2013).
[13] E. A. Brener, M. B. Geilikman, and D. E. Temkin, Zh. Eksp. Teor. Fiz. **94**, 241 (1988) [Sov. Phys. JETP **67**, 1002 (1988)].
[14] F. Liu and H. Metiu, Phys. Rev. E **49**, 2601 (1994).
[15] A. Karma and M. Plapp, Phys. Rev. Lett. **81**, 4444 (1998).
[16] The phase field model has been used to study epitaxial growth of steps. See, for example, Y.-M. Yu and B.-G. Liu, Phys. Rev. E **69**, 021601 (2004); Phys. Rev. B **73**, 035416 (2006); Y.-M. Yu, B.-G. Liu, and A. Voigt, *ibid.* **79**, 235317 (2009).
[17] For phase field models of steps with the ES effect, see O. Pierre-Louis, Phys. Rev. E **68**, 021604 (2003); F. Otto, P. Penzler, A. Rätz, T. Rump, and A. Voigt, Nonlinearity **17**, 477 (2004); since our simplified system is equivalent to the two dimensional solidification from the melt if supercooling in the melt is interpreted as the supersaturation of adatoms, the previous studies for solidification from the melt are readily applicable to the present model without resort to the above more realistic phase field models of steps.
[18] A. Karma and W.-J. Rappel, Phys. Rev. E **57**, 4323 (1998).
[19] A. Karma and W.-J. Rappel, Phys. Rev. E **60**, 3614 (1999).
[20] A.-L. Barabási and H. E. Stanley, *Fractal Concepts in Surface Growth* (Cambridge University, Cambridge, 1995).
[21] A. Pimpinelli and J. Villain, *Physics of Crystal Growth* (Cambridge University, Cambridge, 1998).
[22] For example, the velocity of a freely growing intrusion with $W_0/d_0 = 60$ and $\epsilon_4 = 0.05$ is 10% of the velocity in the sharp interface model. See Ref. [18].
[23] The value of the adatom density at the source, $c_0 = 0.5$, corresponds to the case of step growth on the Ga-deposited Si(111) [5]. The noise adopted here, $F_u = 10^{-5}$, is weaker than that in the experiment. The latter may reach $F_u \sim 10^{-1}$. Such strong fluctuation of the atomic size cannot be properly treated by the PM, and we need to use the LM [10] instead.

[24] J. S. Langer, in *Chance and Matter*, edited by J. Souletie, J. Vannimenus, and R. Stora (North Holland, Amsterdam, 1987), pp. 629–711.

[25] E. Brener, H. Müller-Krumbhaar, and D. Temkin, Europhys. Lett. **17**, 535 (1992).

[26] T. Ihle and H. Müller-Krumbhaar, Phys. Rev. E **49**, 2972 (1994).

[27] E. A. Brener, H. Müller-Krumbhaar, and D. Temkin, Phys. Rev. E **54**, 2714 (1996).

[28] I. Bena, C. Misbah, and A. Valance, Phys. Rev. B **47**, 7408 (1993).

[29] M. Sato, M. Uwaha, and Y. Saito, Phys. Rev. Lett. **80**, 4233 (1998).

[30] O. Pierre-Louis, C. Misbah, Y. Saito, J. Krug, and P. Politi, Phys. Rev. Lett. **80**, 4221 (1998).

[31] M. Sato, M. Uwaha, Y. Saito, and Y. Hirose, Phys. Rev. B **65**, 245427 (2002); R. Kato, M. Uwaha, Y. Saito, and H. Hibino, Surf. Sci. **522**, 64 (2003).

[32] S. Paulin, F. Gillet, O. Pierre-Louis, and C. Misbah, Phys. Rev. Lett. **86**, 5538 (2001).

[33] M. Sato, M. Uwaha, Y. Saito, and Y. Hirose, Phys. Rev. B **67**, 125408 (2003).

[34] G. Danker, O. Pierre-Louis, K. Kassner, and C. Misbah, Phys. Rev. E **68**, 020601(R) (2003).

[35] P. Politi and C. Misbah, Phys. Rev. Lett. **92**, 090601 (2004).

[36] In the LM, the noise is intrinsically strong and uncontrollable, and then the growing step takes a fractal form at a high velocity [10]. The maximum velocity $V_{\rm D}$ of a fractal step is determined by the diffusion length related to this pattern. As a function of the density at the source c_0, it is given by [25] $V_{\rm D} \sim c_0^{2/(d-d_{\rm f})} \sim c_0^{7.0}$, which is seen in Fig. 9(b) of Ref. [10] in the low-density part. In Ref. [10], it is erroneously argued that the exponent is $1/(d - d_{\rm f})$, which looks to be consistent with the data in high density, but only accidentally.

[37] It was not possible to fully verify the statement numerically because of the rapid increase of Λ.

[38] The coefficient in Eq. (A.10) cannot be determined for $n = 4$ in the same way as for $n = 2$. In our simulation we have checked the relation (A.10) is valid for an equilibrium situation (as demonstrated in Ref. [19]).